Silicon Oxide Surface as a Substrate of Polymer Thin Films

K. Shin,[†,§] X. Hu,[†] X. Zheng,[†] M. H. Rafailovich,[*,†] J. Sokolov,[†] V. Zaitsev,[‡] and S. A. Schwarz[‡]

Department of Materials Science and Engineering, State University of New York at Stony Brook, Stony Brook, New York 11794-2275, and Department of Physics, Queens College of the City University of New York, Flushing, New York 11367

Received October 26, 2000; Revised Manuscript Received April 9, 2001

ABSTRACT: We have measured the thickness of the oxide layer of Si wafers as a function of annealing temperature following treatment with either a modified Shiraki method (hydrophilic) or HF etching (hydrophobic). The results show that in both cases there exists a well-defined oxide layer, approximately 20 Å thick, which forms within at least 20 min of the processing. The density of this layer is initially 35% of the usual silicon oxides. The density of this layer gradually increases, approaching that of the pure oxides as the substrates are annealed from room temperature to 180 °C. These results were interpreted in terms of a complexed layer of water. These results are consistent with dynamic secondary ion mass spectrometry, which shows that the amount of oxygen at the Si interface decreases with increasing temperature. The activation energies, obtained 31.6 and 19.3 kJ/mol for the hydrophilic and hydrophobic surfaces, are consistent with the evaporation energy of water. The effect of the adsorbed water was also evident on the diffusion coefficient of PS from the Si interface. The diffusion coefficient (D^*) was expressed as $D^* = D_{WLF}(T) \exp(-\Delta E_s/kT)$ where D_{WLF} is the usual WLF temperature dependence diffusion coefficient, and the additional activation energy measured was $\Delta E_s \sim 6.7$ kJ/mol per contact. The energy corresponds to the interaction energy between styrene monomers and mostly the adsorbed water layer.

Introduction

Numerous papers have discussed the effect of the polymer/substrate interface on inducing orientation in block copolymers,[1] promoting wetting/dewetting,[2−5] and affecting polymer dynamics and adsorption[6,7] as well as the glass transition.[8,9] The preferential segregation of polymer chains has been observed,[10] and Zheng et al. reported long-range effects on polymer diffusion by the substrate.[11] Since the effects on the fluid properties of polymer thin films, which originate at the polymer/substrate interface, can be substantial, the understanding of these substrates is of importance. Si wafers are the most preferred substrates for studying polymer thin films since they can be cleaned, polished atomically flat, and cleaved easily. In addition as is well established in the electronic industry, control of oxidation provides a great versatility to the silicon substrate. Etching the oxide layer and passivating it with hydrogen leads to a hydrophobic surface. A hydrophilic surface can be produced by growing a variety of different oxides. The Si surface is also readily oxidized under normal ambient conditions, since atmospheric oxygen and moisture are known to be major oxidation sources.[12] As was first shown by Frantz and Granick,[13] different surface treatments can significantly modify significantly the physics of the polymer/substrate interface.

Due to intense industrial interest in semiconductor devices, many studies of the silicon and silicon oxide surfaces have already been performed.[12,14−19] Due to low glass transition temperatures for polymers and the incapability of spin coating under ultrahigh vacuum, it is therefore important to study the silicon surface under conditions applicable to polymer film processing.

In this article, we present studies characterizing the nature of the silicon surface after different treatments, including HF stripping, chemical oxidation, and baking in a vacuum and the associated rheological properties of polymer thin films. We measure thickness changes by X-ray reflectivity (XR) as a function of annealing temperature, and these results will be correlated with secondary ion mass spectrometry (SIMS) measurements of the diffusion of polymer films.

Experimental Section

Si wafers were cleaved into to 0.5 in. × 0.5 in. squares and sonicated in trichloroethylene, methanol, and deionized (DI) water for 3 min. The samples were dried in N_2 gas before each immersion in the different solvents.

The samples were then subjected to the following cleaning procedures: First, to remove any remaining organic contaminants, samples were immersed in freshly mixed ammonia−peroxide solution ($NH_4OH:H_2O_2:H_2O$, v:v:v = 1:1:3) for 15 min at about 100 °C. One can see vigorous bubbling of oxygen. The samples were then rinsed in deionized (DI) water. As a postcleaning check, water wetting is a good indicator. When the surface is uniformly cleaned, the water layer will wet without breaking on the surface. It is best to proceed with the Shiraki method at this point. One can store the wafer pieces in water for future use, but one should be aware that removing the wafer from the water without picking up contaminants from the water surface can be very tricky. Typical "oxide layers " up to 100 Å thick have been observed on wafers removed from water after storing in water for 3 days.[20] Immersing in very dilute hydrofluoric acid solution ($HF:H_2O$, v:v = 1:10) for 3 min followed by subsequent rinsing in DI water, for 2 min, can remove this thick oxide layer.

To get a uniform oxide layer, chemical oxidation is necessary. We apply the modified Shiraki technique[21,22] which removes any ionic/metallic impurities and has been shown to create a thin oxide layer (∼20 Å). A sulfuric acid solution ($H_2SO_4:H_2O_2:H_2O$, v:v:v = 1:1:3) is mixed, and the silicon pieces are immersed for 15 min while heated to ∼100 °C, while oxygen bubbles strike the surface strenuously.

To produce a hydrophobic Si surface, buffered oxide etching solution has been used. To prepare this solution, ammonium

[†] SUNY at Stony Brook.
[‡] QC of CUNY.
[§] Current address: NCNR, NIST, Gaithersburg, MD 20899-8562.
* Corresponding author. Tel 631-632-8483, e-mail miriam.rafailovich@sunysb.edu.

10.1021/ma001846q CCC: $20.00
Published on Web 06/07/2001

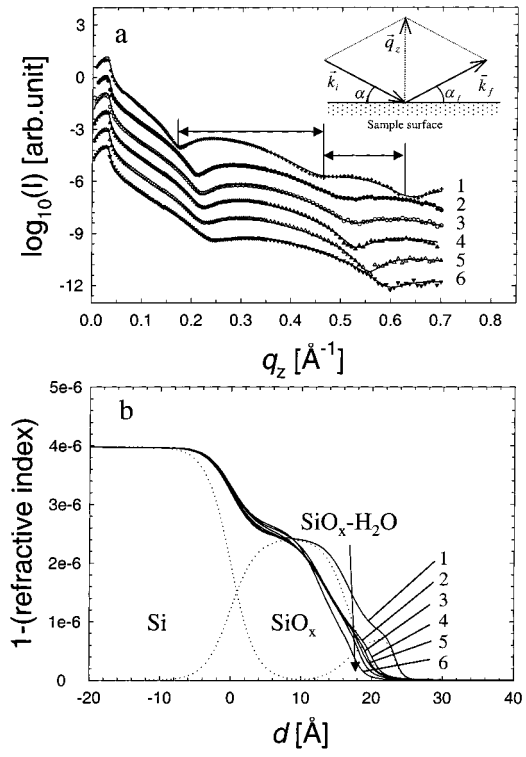

Figure 1. (a) X-ray reflectivity curves as a function of annealing temperature for a chemically oxidized Shiraki silicon surface. Solid lines are best fits. 1 (RT), 2 (60 °C), 3 (90 °C), 4 (120 °C), 5 (150 °C), 6 (180 °C). The arrows indicate nonuniform oscillation periods. The curves were offset by a constant for easier viewing. (inset) The scattering geometry of the X-ray experiments. The momentum vector transfer is defined by $\vec{q}_z = \vec{k}_f - \vec{k}_i$ where $\vec{k}_i$ and $\vec{k}_f$ are the incident and exit wave vectors. (b) The solid line is the total dispersion profile used to obtain the fits in (a). The dashed lines indicate respective layer profiles of Si, the layer **1** (SiO_x:H_2O), and the layer **2** (H_2O:vacuum).

fluoride solution (NH_3F:H_2O, v:v = 1:1.25) and HF (49%) are mixed in the ratio of 6:1. The wafers can be immersed for 2−3 min. It should be noted that NH_3F could easily pick up atmospheric contaminants. Hence, if spectroscopic grade is not available, then very dilute HF solution (HF:H_2O, v:v = 1:10) can substitute for this buffered solution. To obtain a moisture-free surface, a baking procedure is proposed. After rinsing in water and drying in N_2 gas, the wafer pieces were put in a high vacuum oven for 3 h at 200 °C.

Immediately after cleaning the samples were mounted in a specially designed sample chamber, allowing to temperature control up to 220 °C under high vacuum ($\sim 10^{-6}$ Torr). The cell was designed with Kapton windows, which allowed in-situ X-ray measurement while varying the temperature and annealing times.

X-ray specular reflectivity (XR) was used to monitor the in-situ changes of the oxide layers as a function of annealing of the Si wafers. The measurements were performed at the beamline X10B, the National Synchrotron Light Source, Brookhaven National Laboratory, at an energy of 11 keV, which corresponds to a wavelength of $\lambda = 1.13$ Å. The geometry used for XR is shown in the inset of Figure 1. The specular reflectivity is defined as the intensity taken as a function of the wavevector transfer, q_z, by varying the incident (α_i) and exit (α_f) while maintaining $\alpha_i = \alpha_f$ with $q_z = k(\sin \alpha_i + \sin \alpha_f)$ where k is given by $k = 2\pi/\lambda$. Since the specular reflectivity detects the variation of the electron density $\rho(z)$ in the direction to surface normal, averaged in the parallel plane to the sample surface, it is sensitive to the layer thicknesses (d), the density contrasts, and the interfacial roughnesses (σ_1, σ_2) defined by the probability density.

Depending on their electron densities, the indices of refraction of "oxide layers" are sufficiently different from those of Si complexes. For examples, neglecting absorption, at an incident energy of 11 keV the calculated indices of refraction $n = 1 - \delta$ with dispersion δ of Si, Si−H, Si−OH, and SiO_2 are $n_{Si} = 1 - 4.0377 \times 10^{-6}$, $n_{Si-H} = 1 - 4.17260 \times 10^{-6}$, $n_{Si-OH} = 1 - 4.11582 \times 10^{-6}$, and $n_{SiO_2} = 1 - 3.79978 \times 10^{-6}$, respectively. The δ is given linearly in terms of the electron density, ρ_{el}, by $\delta = \lambda^2 \rho_{el} r_0 / 2\pi$ where r_0 is the classical electron radius. Therefore, the reflected intensity at the interfaces is sensitive to the electron density variation.[23] In this study, XR shows enough resolution to determine the changes of properties of the oxide layer to within a few angstroms. It takes about 30 min for one reflectivity curve, and we wait 20 min to stabilize the temperature between the measurements. To analyze the reflectivity data, the recursive Parratt formalism has been used.[24] Fits were obtained with multilayer box models consisting of electron density, corresponding to layers that contain silicon derivatives, i.e., SiH, SiOH, SiO, and SiO_2 and up to two layers were utilized. The δ, d, and σ were varied for optimization.

Dynamic secondary ion mass spectrometry (DSIMS) was used to monitor the effects of an oxide layer on polymer diffusion, since DSIMS can simultaneously measure both oxygen and deuterium ions. Diffusion of hydrogenated polystyrene (HPS) in deuterated polystyrene (DPS) was measured by DSIMS to determine the tracer diffusion coefficient (D^*) as a function of temperature. Thin films (∼50 Å) of monodisperse polystyrene of M_w = 90 000 g/mol were spin-coated directly onto native oxide covered Si wafers from toluene solution. Thick films (∼4000 Å) of monodisperse deuterated polystyrene (DPS) of M_w = 713 000 were then floated off a glass slide from water onto the PS-covered surface. The PS film thickness of about 50 Å (less than $2R_g$) was chosen to ensure that most chains in the thin layer would initially have some contact points with the Si interface. The deuterated matrix was chosen to eliminate uncertainties in the diffusion profiles due to preferential segregation of DPS to the Si substrate.[10] A control sample to measure the bulk diffusion coefficient was prepared by spinning the thick DPS layer onto the Si surface and floating the thin PS on top of it. The samples were then annealed in a vacuum of 10^{-6} Torr at different temperatures, and the diffusion profiles were determined. The oxygen at the Si interface was profiled simultaneously with the volume fraction vs distance profiles of the diffusing PS layer by rastering a 2 keV Ar^+ ion beam over a 1 mm^2 area and detecting CH^-, CD^-, O, Si, and D^- ion intensities. The data for the polymer-covered substrates were compared to DSIMS data from bare Si annealed at the same temperatures. All samples were covered with a 200 Å PS sacrificial layer for the DSIMS analysis. Further details on the sample geometry and data analysis are given in ref 25. From the O^- ion intensity, the oxygen profiles of a PS-covered sample and a bare substrate are measured as baked at temperatures ranging from 100 to 200 °C.

It should be emphasized that in this study we are interested in the oxide layer that results from various surface treatments that are performed in ambient conditions. Hence, the nature of the oxides may vary from those previously studied in UHV with atomic level monolayer control.[12,15c]

Results and Discussion

In Figure 1a we plot the specular X-ray intensity measurements as a function of q_z for a Si wafer treated with the Shiraki method. The different curves correspond to different annealing temperatures. From the figure we can see that the interference fringes persist to large q the cleaning procedure retains the atomic flatness of the surface. Close examination of the figures shows that the lengths of the oscillation periods, Δq_z, delineated by the arrows in the figure are not uniform. Two distinct oscillations are competing in one scan, which implies that more than one uniform layer is

Table 1. X-ray Reflectivity Fitting Parameters[a]

T (°C)	δ_1 ($\times 10^{-6}$)	σ_1 (Å)	d_1 (Å)	σ_{12} (Å)	δ_2 ($\times 10^{-6}$)	σ_2 (Å)	d_2 (Å)
Figure 1. Shiraki Surface							
22	2.41	3.3	16.5	3.0	0.87	1.4	6.5
60	2.49	3.3	13.9	3.5	0.66	1.7	6.1
90	2.54	3.3	13.5	3.4	0.63	1.5	5.6
120	2.61	3.3	13.6	4.8	0.63	1.3	5.2
150	2.59	3.3	13.3	4.6	0.45	1.2	4.8
180	2.64	3.3	12.5	4.3	0.39	1.4	4.7
Figure 2. HF-Etched Surface							
22	2.64	4.1	20.0	4.4			
50	2.44	4.8	15.7	3.7			
85	2.54	4.8	14.0	3.7			
130	2.75	5.1	13.2	3.5			
160	3.01	5.2	12.8	3.7			
190	3.01	5.3	12.6	3.7			
220	3.14	5.6	12.4	3.7			

[a] The error of d is 1−2 Å. The errors of δ and σ are 10%−15% of the value. d, σ, and δ denote thickness, roughness, and dispersion, respectively, and subscripts 1, 2, and 12 denote layer **1**, layer **2**, and interface between layer **1** and layer **2**, respectively.

present. The model used to obtain a least chi-square fit the data (solid lines) is shown in Figure 1b. The model consists of two oxide layers: a high electron density layer (layer **1**) adjacent to the Si substrate and a second layer of lower electron density at the vacuum interface (layer **2**). The free parameters used in the fits shown as solid lines are thicknesses, d_1 and d_2, roughnesses at the silicon/layer **1**, layer **1**/layer **2**, and air/layer **2** interfaces, σ_1, σ_{12}, and σ_2, and respective X-ray index of refraction of the two layers. From the results tabulated in Table 1, we see that the first layer has $\delta_1 \sim (2.4-2.8) \times 10^{-6}$, which is somewhat lower than $\delta_{SiOH} \sim 4.11 \times 10^{-6}$ or the electron density of any pure silicon oxide or hydride layer. This layer is also consistent with the oxide layer thickness normally reported in numerous other reflectivity studies of annealed polymer films on Si substrates.[26] The layer **2** has a much lower density ($\delta_1 \sim 0.9 \times 10^{-6}$), which is comparable to that of a partial layer of pure water ($\delta_{H_2O} \sim 1.9 \times 10^{-6}$). As temperature is increased (from Figure 1a-2 to Figure 1a-6), one can see that the amplitude of the beating rapidly decreases and the frequency of the Kiessig fringes becomes more uniform.

Figure 1b shows the dispersion (δ) profiles as a function of d or distance from the Si surface which were used to fit the reflectivity data. In the proposed model we assume that the first layer consists of a hydrated Si oxide ($SiO;(H_2O)_x$), $\delta_1 = \phi_{SiO}\,\delta_{SiO} + (1 - \phi_{SiO})\delta_{H_2O}$, where ϕ_{SiO} is the volume fraction of the silicon oxide.[27] On the other hand, the second layer consists of water droplets, i.e., an incomplete layer ($\delta_1 = \phi_{H_2O}\delta_{H_2O} + (1 - \phi_{H_2O})\delta_{vacuum}$). From the figure and Table 1 we can see that the thickness of the first layer decreases abruptly at 60 °C and then remains constant with temperature. On the other hand, the electron density increases, gradually approaching the density of the pure oxides. The electron density of the second layer decreases much faster with increasing temperature. This is consistent with the first layer being composed of water complexed to the oxide surface produced in the Shiraki method and characterized by Boonekamp et al.[17] This layer is relatively strongly bound and requires high temperature to be removed. The second layer is simply a water layer adsorbed onto the first. The adsorption energy for this layer is much lower, and this layer is mostly driven off for $T \leq 60$ °C. Since this temperature is lower than T_g of PS and other polymer commonly studies with reflectivity, this layer has not been detected and is not expected to affect results of films annealed in their liquid state.

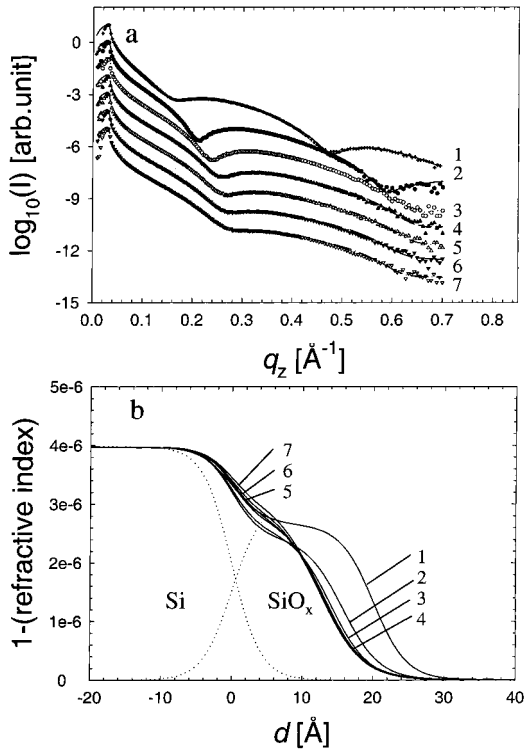

Figure 2. X-ray reflectivity curves as a function of annealing temperature for a HF etched silicon surface. Solid lines are best fits. 1 (RT), 2 (50 °C), 3 (85 °C), 4 (120 °C), 5 (150 °C), 6 (180 °C), 7 (210 °C). The curves were offset by a constant for easier viewing. (b) The solid line is the total dispersion profile used to obtain the fits in (a). The dashed lines indicate respective layer profiles of Si, the layer **1** ($SiH:SiOH:H_2O$).

The X-ray reflectivity curves for a HF-etched sample annealed at different temperatures are shown in Figure 2a. Surprisingly, an oxide layer with significant thickness is observed at room temperature, despite the fact that the surface is highly hydrophobic. Previous studies of HF-etched surface where hydrogen passivation was postulated were done in UHV conditions.[12,15,18] These surfaces were shown not to be stable in air for times longer than a few minutes.[17,18,28] The processing of polymer films is usually much longer than that, allowing sufficient time oxides and water to readsorb to the surface, which is consistent with the observed oxide layer. In contrast to the Shiraki surface, the HF-etched surface exhibits only one periodic oscillation corresponding to a single oxide layer of approximate the thickness, $d = 2\pi/\Delta q_z \sim 20$ Å. The detailed model is shown in Figure 2b. From the figure we can see that on this surface as well, the layer gets abruptly thinner when annealed at $T \leq 60$ °C. The thickness then remains fairly constant around $d \sim 14$ Å, while the electron density is observed to increase. The electron density of this layer $\delta \sim (2.64-3.14) \times 10^{-6}$ is still significantly less than $\delta_{SiH} \sim 4.17 \times 10^{-6}$ of SiH or $\delta_{SiOH} \sim 4.11 \times 10^{-6}$ of SiOH.[29] If we model this layer, a single layer of a mixture ($\delta = \delta_{\langle SiH:SiOH \rangle}$) of hydrogen passivated (Si−H) and hydride (Si−OH), and complexed with water as we did for the Shiraki surface, is proposed with a density profile of $\delta_1 = \phi_{SiH}\,\delta_{\langle SiH:SiOH \rangle} + (1 - \delta_{\langle SiH:SiOH \rangle})\delta_{H_2O}$.

In Figure 3 we plot the fraction of silicon derivatives,

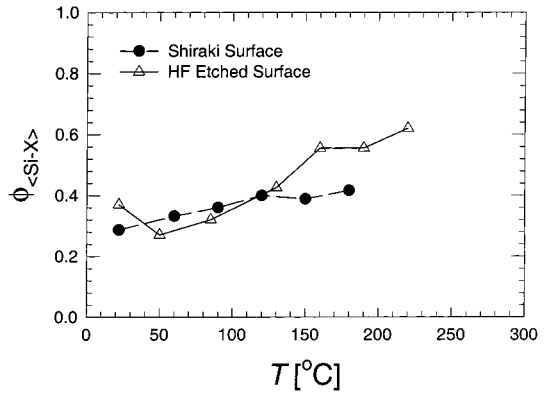

Figure 3. Volume fraction profiles of silicon complexes in the layer **1** of a HF etched (●) and a Shiraki (△) surface. The values at *y*-axis are representing the obtained electron densities normalized by the average electron density of silicon derivatives, SiH, SiOH, and SiO.

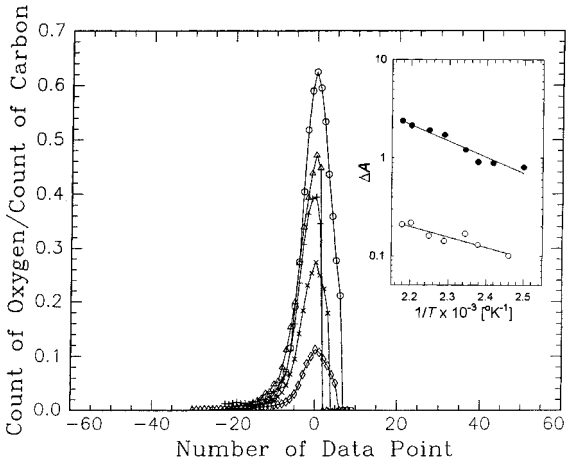

Figure 4. Normalized oxygen profile at the Si interface vs channel numbers. The surfaces were annealed for 10 h at 120 °C (○) and 133 °C (△), 2 h at 147 °C (+) and 163 °C (×), and 2 min at 200 °C (◇). (inset) The linearly reducing difference between the area of oxygen peak from a surface annealed at 120 °C and areas of surfaces annealed at various temperatures ranging from 100 to 190 °C as a function of inverse temperature (K^{-1}). The bare silicon surface with native oxide (●) and PS-covered silicon surface (○) are measured.

$\phi_{\langle Si-X\rangle}$, as a function of annealing temperature, where X is the atoms that are chemically bonded to the silicon surface. When $\phi_{\langle Si-X\rangle} = 1$, the electron density of this layer has that of a water-free surface. As mentioned previously, the main difference between the HF and Shiraki surfaces consists of the absence of the adsorbed water layer. This is consistent with the large difference in hydrophobicities of the two surfaces. From the figure one can see that the complexed water (layer **2**) is driven off somewhat more quickly than the HF surface, indicating that the chemical nature of the two surfaces may be different.

The activation energy for desorption of the adsorbed moisture was found by monitoring the surface oxygen signal in the dynamic SIMS measurements of polymer interdiffusion described below. The height of the oxygen count rate normalized by the carbon count rate is plotted in Figure 4. We can assume an *Arrhenius* equation,[30] for thermal activation given by

$$\Delta A = C \exp\left(-\frac{\Delta E^*}{kT}\right) \qquad (1)$$

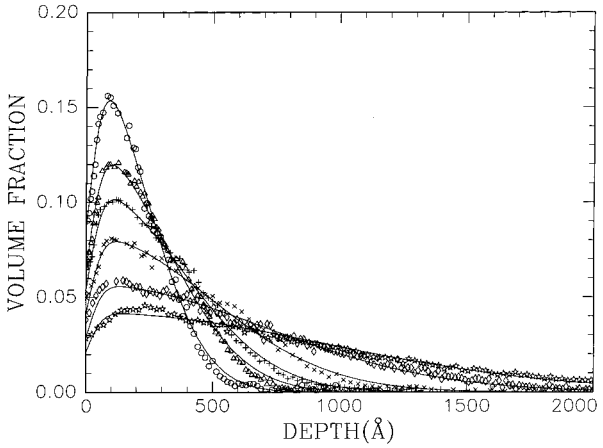

Figure 5. SIMS depth profiles obtained from the CH^- ion concentration of a PS (M_w = 90 000 g/mol) layer and allowed to diffuse into a DPS (M_w = 713 000 g/mol) interface at 120 (○), 133 (△), 147 (+), 163 (×), 181 (◇), and 191 °C (☆). The solid lines are from the fits to eq 2.

where a layer of a given area (A) is at equilibrium on the surface at a given temperature, then ΔA is exponentially related to the Boltzmann constant k, the temperature T (K), and the activation energy ΔE^* with a constant C. In the inset to Figure 4, we plot the log of difference in the area under the normalized oxygen peak at T = 120 °C and that at other temperatures ΔA (T) vs the reciprocal of the absolute temperature $1/T$ (K^{-1}). The open and solid circles represent the PS-covered hydrophobic silicon surface and the bare silicon surface with a native oxide, respectively. We can see a linear dependence with slopes -3.21×10^2 and -6.83×10^1 for the hydrophilic and hydrophobic surfaces, respectively. We can extract the activation energies ΔE^* of both cases, 31.6 and 19.3 ± 2 kJ/mol. These values are comparable to the latent heat of vaporization of water or L_{vap} = 40.7 kJ/mol and much smaller than what would be necessary to break an Si−O bond, ∼370 kJ/mol.[31] In addition, the desorbing of moisture still occurs even under polymer thin films, and water molecules on the oxide layer diffused out through the permeable polymer thin film.

To determine the effects of the oxide layer on the rheological properties of polymer films, we measured the tracer diffusion coefficient of polystyrene thin films adjacent to a Shiraki surface. It should be noticed that since $T_g \sim 100$ °C for PS we can only probe the effect of the strongly comlexed layer since the weakly adsorbed layer of water is completely removed for $T \leq 60$ °C. Figure 5 shows the DSIMS spectra of a 50 Å HPS (M_w = 90 000 g/mol) layer allowed to diffuse into a bulk DPS layer (M_w = 713 000 g/mol) after annealing at various temperatures and times. The solid lines are fits to an error function equation for the Fickian diffusion for a thin film of thickness h, diffusing into a semiinfinite medium given by[32]

$$\phi(x) = 0.5 \operatorname{erf}\left[\frac{h - x}{\sqrt{4D^*t}}\right] + 0.5 \operatorname{erf}\left[\frac{h + x}{\sqrt{4D^*t}}\right] \qquad (2)$$

where D^* and t are the tracer diffusion coefficient and annealing time, respectively. The values of log D/T^* are plotted as a function of temperature in Figure 6 (solid circles). The open triangle corresponds to the diffusion 'bulk" diffusion coefficient measured at 153 °C. These values are compared with the predictions of the Wil-

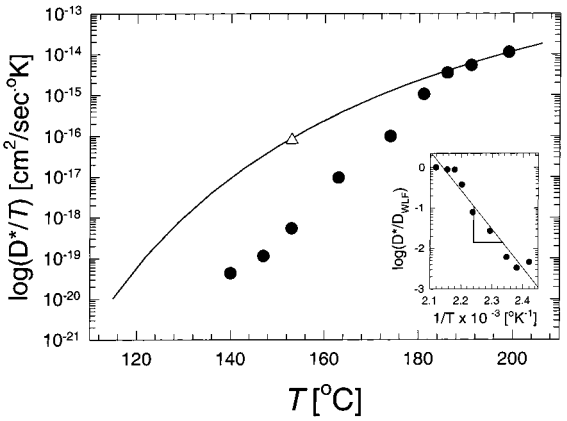

Figure 6. Temperature dependence of tracer diffusion coefficient of polystyrene of $M_w = 90\,000$ g/mol near attractive silicon oxides interfaces. Solid symbols (●) are experimental data. The solid line is obtained by the WLF equation for polystyrene. The triangle is the measured bulk diffusion coefficient. (inset) Temperature (K) dependence of the normalized diffusion coefficients (D^*/D). The slope indicates the thermal activation energy for the diffusion near Si surface ($\Delta E_s/k$).

liams−Landel−Ferry (WLF)[33] scaling for PS.[34] From the figure we can see that the surface diffusion coefficients are much lower than those predicted by WLF for $T <$ 160 °C and with a weaker temperature dependence. For $T >$ 160 °C the temperature dependence becomes much steeper than WLF, so that at $T \sim$ 180 °C the bulk and surface diffusion coefficients coincide. These results show that the slower dynamics that have been reported by several groups are correlated to interactions between the polymer film and the complexed water layer in the silicon oxide layer. As the water is desorbed with increasing annealing temperature, the effect of the surface on the dynamics decreases.

These results can be understood quantitatively if we model the diffusion away from the silicon interface as an activated process that requires an additional activation energy term, ΔE_s. As similarly expressed in eq 1, in this case the diffusion coefficient is given by

$$D^* = D_{WLF}(T) \exp\left(-\frac{\Delta E_s}{kT}\right) \qquad (3)$$

where $D_{WLF}(T)$ is the bulk diffusion coefficient given by the WLF scaling. In the inset of Figure 6 we plot log-($D^*/D(T)$) vs $1/T$ (K^{-1}) for the data shown in Figure 6. From the slope we obtain a value of $\Delta E_s = 202.5$ kJ/mol. Since D^* is the center-of-mass diffusion coefficient of an entire polymer chain, ΔE_s corresponds to the activation energy of removing the whole chain from the attractive interface. If we make the naive assumption that a polymer molecule has at least $N^{1/2}$ segments contacting the surface, we can estimate the maximum strength of single surface−polymer bond. For a chain of $N = 900$ is approximately $\Delta E_s \sim 6.7$ kJ/mol. This value is larger than the van der Waals interaction energy (∼1 kJ/mol) but still much smaller than the typical values for hydrogen bonding or 10−40 kJ/mol.[31]

Conclusions

In conclusion, we have measured the thickness of the oxide layer of Si wafers as a function of annealing temperature following treatment with either a modified Shiraki method or HF etching. The results show that in both cases there exists a well-defined oxide layer, approximately 20 Å thick, which forms within at least 20 min of the processing. The density of this layer is initially 35% of the usual silicon oxides. The density of this layer gradually increases, approaching that of the pure oxides as the substrates are annealed from room temperature to 180 °C. These results were interpreted in terms of a comlexed layer of water. These results are consistent with dynamic SIMS which show that the amount of oxygen at the Si interface decreases with increasing temperature. The activation energy obtained, 31.6 and 19.3 kJ/mol for the hydrophilic and hydrophobic surfaces, is consistent with the energy of evaporation of water. The effect of the adsorbed water was also evident on the diffusion coefficient of PS from the Si interface. The diffusion coefficient (D^*) was expressed as $D^* = D_{WLF}(T) \exp(-\Delta E_s/kT)$ where D_{WLF} is the usual WLF temperature dependence diffusion coefficient, and the additional activation energy measured was $\Delta E_s \sim$ 6.7 kJ/mol per contact. The energy corresponds to the interaction energy between styrene monomers and mostly the adsorbed water layer.

Acknowledgment. This work was supported by NSF-MRSEC Program No. DMR0080604. The authors thank R. Kolb (ExxonMobil R& E Co.) and S. Bennett (BNL) for generous assistance with the instrumental support. Parts of research were carried out at the National Synchrotron Light Source, Brookhaven National Laboratory, which is supported by the U.S. Department of Energy, Division of Materials Sciences and Division of Chemical Sciences.

References and Notes

(1) Anastasiadis, S. H.; Russell, T. P.; Satija, S. K.; Majkrzak, C. F. *Phys. Rev. Lett.* **1989**, *62*, 1852.
(2) Reiter, G. *Phys. Rev. Lett.* **1991**, *65*, 75.
(3) Geoghegan, M.; Nicolai, T.; Penfold. J.; Jones, R. A. L. *Macromolecules* **1997**, *30*, 4220.
(4) Zhao, W.; Rafailovich, M. H.; Sokolov, J.; Fetters, L. J.; Plano, R.; Sanyal, M. K.; Sinha, S. K.; Sauer, B. B. *Phys. Rev. Lett.* **1993**, *70*, 1453.
(5) Shull, K. R. *Faraday Discuss.* **1994**, *98*, 203.
(6) Zheng, X.; Sauer, B. B.; van Alsten, J. G.; Schwarz, S. A.; Rafailovich, M. H.; Sokolov, J.; Rubinstein, M. *Phys. Rev. Lett.* **1995**, *74*, 407.
(7) Wang, J.; Tolan, M.; Seeck, O. H.; Sinha, S. K.; Bahr, O.; Rafailovich, M. H.; Sokolov, J. *Phys. Rev. Lett.* **1999**, *83*, 564.
(8) Keddi, J. L.; Jones, R. A. L.; Cory, R. A. *Europhys. Lett.* **1994**, *27*, 59.
(9) Wallace, W. E.; van Zanten, J. H.; Wu, W. L. *Phys. Rev. E* **1996**, *52*, R3329.
(10) (a) Strzhemechny, Y. M.; Schwarz, S. A.; Schachter, J.; Rafailovich, M. H.; Sokolov, J. *J. Vac. Sci. Technol. A* **1997**, *15*, 894. (b) Geoghegan, M.; Nicolai, T.; Penfold, J.; Jones, R. A. L. *Macromolecules* **1997**, *30*, 4220.
(11) Zheng, X.; Rafailovich, M. H.; Sokolov, J.; Strzhemechny, Y.; Schwarz, S. A.; Sauer, B. B.; Rubinstein, M. *Phys. Rev. Lett.* **1997**, *79*, 241.
(12) Weldon, M. K.; Stefanov, B. B.; Raghavachari, K.; Chabal, Y. J. *Phys. Rev. Lett.* **1997**, *79*, 2851.
(13) Frantz, P.; Granick, S. *Langmuir* **1992**, *8*, 1176.
(14) Yablonovitch, E.; Allara, D. L.; Chang, C. C.; Gmitter, T.; Bright, T. B. *Phys. Rev. Lett.* **1986**, *57*, 249.
(15) (a) Higashi, G. S.; Chabal, Y. J.; Trucks, G. W.; Raghavachari, K. *Appl. Phys. Lett.* **1990**, *56*, 656. (b) Trucks, G. W.; Raghavachari, K.; Higashi, G. S.; Chabal, Y. J. *Phys. Rev. Lett.* **1990**, *65*, 504. (c) Stefanov, B. B.; Gurevich, A. B.; Weldon, M. K.; Raghavachari, K.; Chabal, Y. J. *Phys. Rev. Lett.* **1998**, *81*, 3908. (d) Burrow, V. A.; Chabal, Y. J.; Higashi, G. S.; Raghavachari, K.; Christman, S. B. *Appl. Phys. Lett.* **1988**, *53*, 998.
(16) Himpsel, F. J.; Mcfeely, F. R.; Talebibrahimi, A.; Yarmoff, J. A.; Hollinger, G. *Phys. Rev. B* **1988**, *38*, 6084.

(17) Boonekamp, E. P.; Kelly, J. J.; Vandeven, J.; Sondag, A. H. M. *J. Appl. Phys.* **1994**. *75*, 8121.
(18) Neuwald, U.; Feltz, A.; Memmert, U.; Behm, R. J. **1995**, *79*, 4131.
(19) Graf, D.; Grundner, M.; Schulz, R. *J. Vac. Sci. Technol. A* **1989**, *7*, 808.
(20) Shin, K.; Hu, X.; Rafailovich, M. H.; Sokolov, J.; Kolb, R.; Schwarz, S. A.; Strechmechny, Y. *Abstr. Pap. Am. Chem. Soc.* **1999**, *218*, 107-COLL.
(21) Jaeger, R. C. *Introduction to Microelectronic Fabrication*; Addison-Wesley: Reading, MA, 1993; Vol. 5.
(22) Kern, W.; Puotinen, D. A. *RCA Rev.* **1970**, *31*, 187.
(23) Russell, T. P. *Mater. Sci. Rep.* **1990**, *5*, 171.
(24) Parratt, L. G. *Phys. Rev.* **1954**, *95*, 359.
(25) Schwarz, S. A.; Winkens, B. J.; Pudensi, M. A. A.; Rafailovich, M. H.; Sokolov, J.; Zhao, X.; Zhao, W.; Zheng, Z.; Russell, T. P.; Jones, R. A. L. *Mol. Phys.*, **1992**, *76*, 937.
(26) Tolan, M. *X-ray Scattering from Soft-Matter Thin Films;* Springer Tracts in Modern Physics; Springer: Berlin, 1999; Vol. 148.
(27) To identify the specific oxide, further FT-IR measurement is necessary.
(28) Higashi, G. S., private communication.
(29) Since the electron densities of SiH and Si−OH, or SiO_x are similar, we cannot differentiate between them (ref 27).
(30) Barrett, C. R.; Nix, W. D.; Tetelman, A. S. *The Principles of Engineering Materials*; Prentice Hall: Englewood Cliffs, NJ, 1973.
(31) Israelachvili, J. *Intermolecular & Surface Forces*, 2nd ed.; Academic Press: San Diego, 1991.
(32) Crank, J. *The Mathematics of Diffusion*, 2nd ed.; Oxford Science Publication: New York, 1998.
(33) Ferry, J. D. *Viscoelastic Properties of Polymers*, 2nd ed.; Wiley: New York, 1970; p 315.
(34) Green, P. F.; Kramer, E. J. *J. Mater. Res.* **1986**, *1*, 202.

MA001846Q